Communications Research Centre

AN EXPERIMENTAL LOOK AT THE USE OF RADAR TO MEASURE SNOW AND ICE DEPTHS

by

G.O. Venier and F.R. Cross

DEPARTMENT OF COMMUNICATIONS
MINISTÈRE DES COMMUNICATIONS

CRC TECHNICAL NOTE NO. 646

CANADA

OTTAWA, NOVEMBER 1972

COMMUNICATIONS RESEARCH CENTRE

DEPARTMENT OF COMMUNICATIONS
CANADA

AN EXPERIMENTAL LOOK AT THE USE OF RADAR TO MEASURE SNOW AND ICE DEPTHS

by

G.O. Venier and F.R. Cross

(Communication Systems Directorate)

CRC TECHNICAL NOTE NO. 646

Received November 1972
Published November 1972
OTTAWA

72-490

TABLE OF CONTENTS

AN EXPERIMENTAL LOOK AT THE USE OF RADAR TO MEASURE SNOW AND ICE DEPTHS

by

G.O. Venier and F.R. Cross

ABSTRACT

The feasibility of using a high resolution FM radar at X-band for measuring the depth of snow and the thickness of fresh water ice was investigated in a series of laboratory and field measurements. A resolution of less than one foot was achieved with the simple radar assembled for the measurements, and it should be possible to reduce this to a few inches in a carefully designed radar. Although only a limited range of snow and ice conditions were available for measurement the results indicated that accurate depth measurements can be carried out with a radar of this type for the conditions encountered and very likely for most other conditions. Finally, some of the parameters of a practical airborne radar system for measuring snow and ice depths are discussed.

1. INTRODUCTION

This report describes a short-term project carried out by the Radar Systems Engineering Section of the Communications Research Centre, to determine experimentally the feasibility of measuring the depth of snow and the thickness of fresh-water ice by radar sensing. Theoretical investigations by Mr. G.M. Royer of this Section (not yet published) have shown, that at X-band, reflections of adequate amplitude should occur from the interfaces in question, and that attenuation of the wave through the snow and ice should not be excessive. X-band was considered the best choice for RF frequency since it would be difficult to achieve the required range resolution at lower frequencies, while at higher frequencies, attenuation in the snow and ice becomes significant, and signals are harder to generate. The experimental program was intended to verify the theoretical results, and to investigate

the practical problems involved in such a high resolution radar. It should be noted, however, that only a very limited effort was available and that consequently, only a 'quick look' was possible using readily available equipment.

A radar of sufficient range resolution to resolve the returns from the surface of the snow and from the ground below was required. A normal pulse radar with such resolution would require a pulse length of one nanosecond or less. The generation of such a pulse and display of the return would be extremely difficult. For this reason, a linearly-frequency-modulated radar was assembled and used for the measurements. While such a radar requires the same RF bandwidth as a short-pulse radar, the signal bandwidth is generated by a relatively slow frequency sweep, and the received signal is converted to one of relatively small bandwidth early in the system.

Since this experimental radar was intended for use in a fixed position above the snow, the time duration of the frequency sweep could be very long, and the processing of the signal could take place over a very long time period including many sweeps. As will be shown later, however, an airborne system must make its measurement in a time over which the aircraft moves only a short distance and this limits the allowable time for a frequency sweep, as well as the processing period.

2. DESCRIPTION OF RADAR

In an FM radar the range can be determined from the frequency difference between the transmitted signal, whose frequency is a linearly increasing function of time, and the received waveform which is a delayed version of it. This is illustrated in Figure 1 for a single point target. The difference frequency, f_d, is proportional to the time delay between the transmitted and received signals. Therefore, if the spectrum of the signal formed by heterodyning the transmitted and received signals is computed and plotted, the result will be a presentation of amplitude as a function of range. The time delay resolution capability of such a system is approximately the inverse of the swept frequency range. Thus, a large RF bandwidth is required for high resolution.

A block diagram of the experimental FM radar which utilizes this technique is shown in Figure 2. The frequency-swept waveform is generated by the sweep generator, amplified by the travelling wave tube amplifier and fed to the horn antenna via ports 1 and 2 of the circulator. The received signals from the horn antenna are passed to an RF bandpass filter and detector via ports 2 and 3 of the circulator. The bandpass filter restricts the used portion of the sweep to approximately 1 GHz and shapes the spectrum to reduce range sidelobes. It would be better to restrict the bandwidth before transmission, but for this experimental system, it was more convenient to do it after reception. The local oscillator signal is derived from the transmitted signal leakage between ports 1 and 3 in the circulator. The leakage signal and the target return signals are heterodyned in the detector and the difference frequency is amplified in the video amplifiers and filtered. The high-pass filter removes the low frequency components of the signal which correspond to very short ranges. The wave analyzer scans slowly through the resultant signal

spectrum and produces a frequency versus time output that is plotted by the pen recorder. Since there is a linear relationship between frequency and range, the resultant display shows signal amplitude as a function of range.

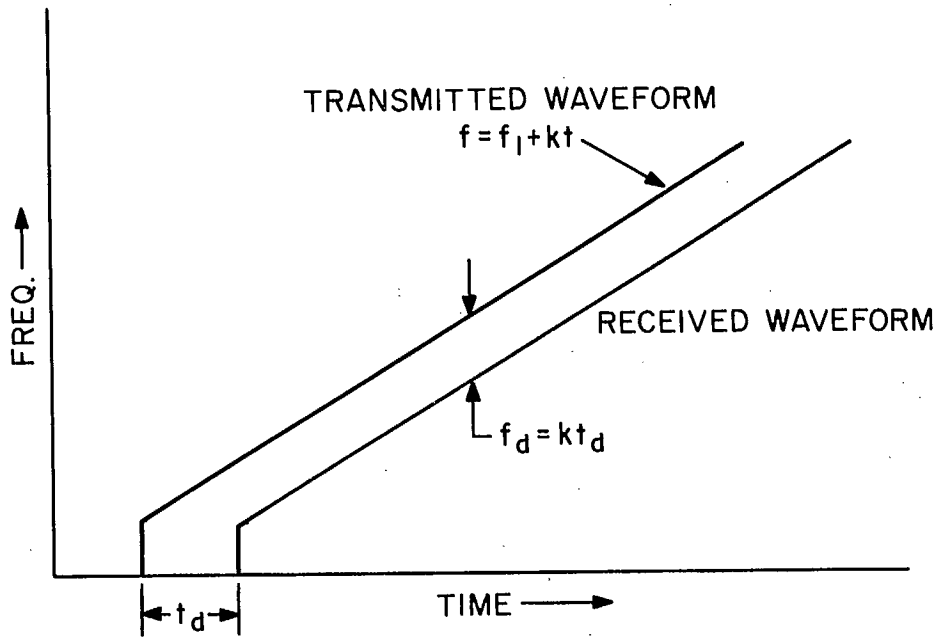

Fig. 1. Frequency difference as a function of time for a single point target.

In this system the transmitted waveform was swept over a frequency range of 8 to 12 GHz in 400 milliseconds, or 10 Hz per nanosecond. Since the two-way signal delay is approximately one nanosecond per foot, the difference frequency is approximately 20 Hz per foot of range (range is defined as the distance between antenna and target, and is therefore one-half the total path length). The transmitted signal is repetitive and the analyzer scan rate was adjusted to scan about one frequency resolution width for each transmitted frequency sweep. Thus, many seconds were required to generate a complete range presentation. Since the received signal is present for only about one quarter of each 400 ms RF sweep, the wave analyzer output peaks during this time about every one-half second. Some capacitance was used across the pen recorder to smooth out this effect, but some fluctuations can still be seen on the records.

2.1 RADAR PERFORMANCE

The resolution of the radar was measured in the laboratory by using two Luneberg lenses as radar reflectors. These are shown in Figure 3. A Luneberg lens was positioned 15 feet from the horn antenna and a second lens was positioned 15 inches behind and to the side of the first lens. These two targets, shown in Figure 4 at A and B, were clearly resolved with a 15 inch target separation. The fluctuations mentioned in the previous paragraph can be seen superimposed on the signal. They have a period of about one-third of a division. The lenses could still be resolved when less than one foot apart. The horn antenna had a gain of 22 dB and a beamwidth of approximately 16°.

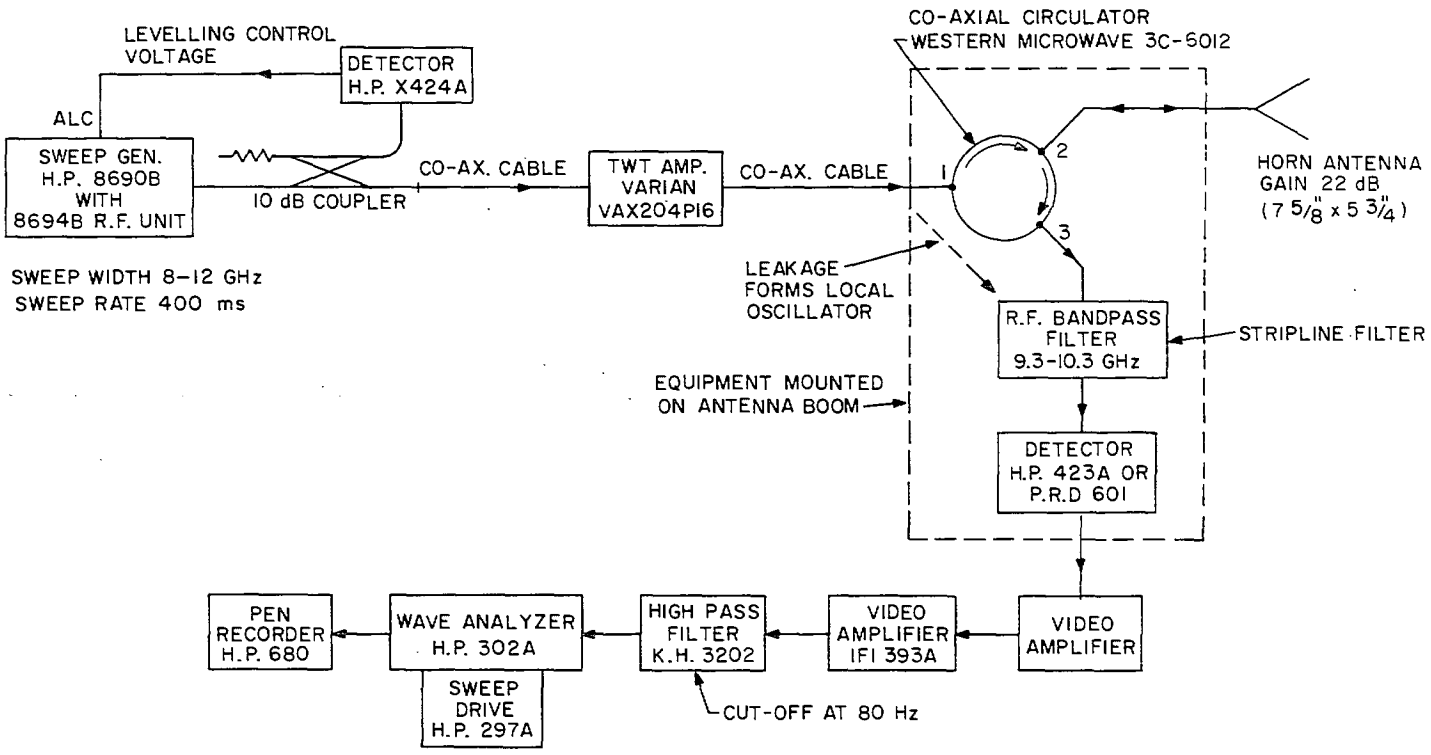

Fig. 2. Block diagram of radar.

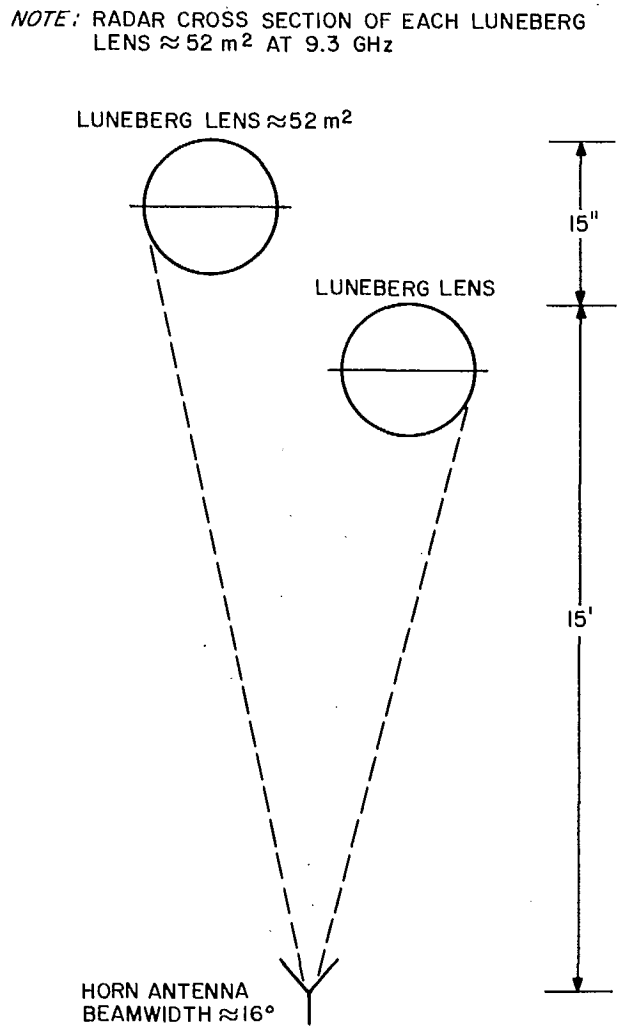

Fig. 3. Radar calibration set-up, Luneberg lenses as targets.

The antenna was mounted on a wooden boom and suspended from the third floor window ledge approximately 34.5 feet above the ground. This is shown in Figure 5. The snow depth under the antenna is shown as a function of distance from the building wall. A maximum snow depth of 39 inches occurred at a distance of 10 feet from the wall. Directly under the antenna 3 feet from the wall, the snow depth was 15 inches.

Fig. 4. Data record of two Luneberg lens targets.

Figure 6 shows an actual recording obtained with the antenna mounted in the third floor window and illuminating the snow below the window. Each small division on the recording corresponded to a range of six inches. Significant target echoes were received from the first and second floor window ledges and smaller echoes were received from the steel frames and screens of both windows. A longer boom for the antenna would have reduced these echoes but this was not considered worthwhile for these first measurements. The two target echoes at the bottom of the recording are approximately 15 inches apart and correspond to the surface of the snow and the ground beneath the snow. The range of the return echo from the snow surface was verified by placing a Luneberg lens on the snow surface. The large return signal from the lens indicated the range of the snow surface from the radar. The snow depth under the antenna was verified by conventional means.

Two types of detectors were used in the radar for the measurements described in this report: a HP423A wideband detector (0.01 - 12.4 GHz) and a PRD601 narrowband detector (8.0 - 10.0 GHz). Unless otherwise specified, the wideband detector was fitted to the radar for the measurements.

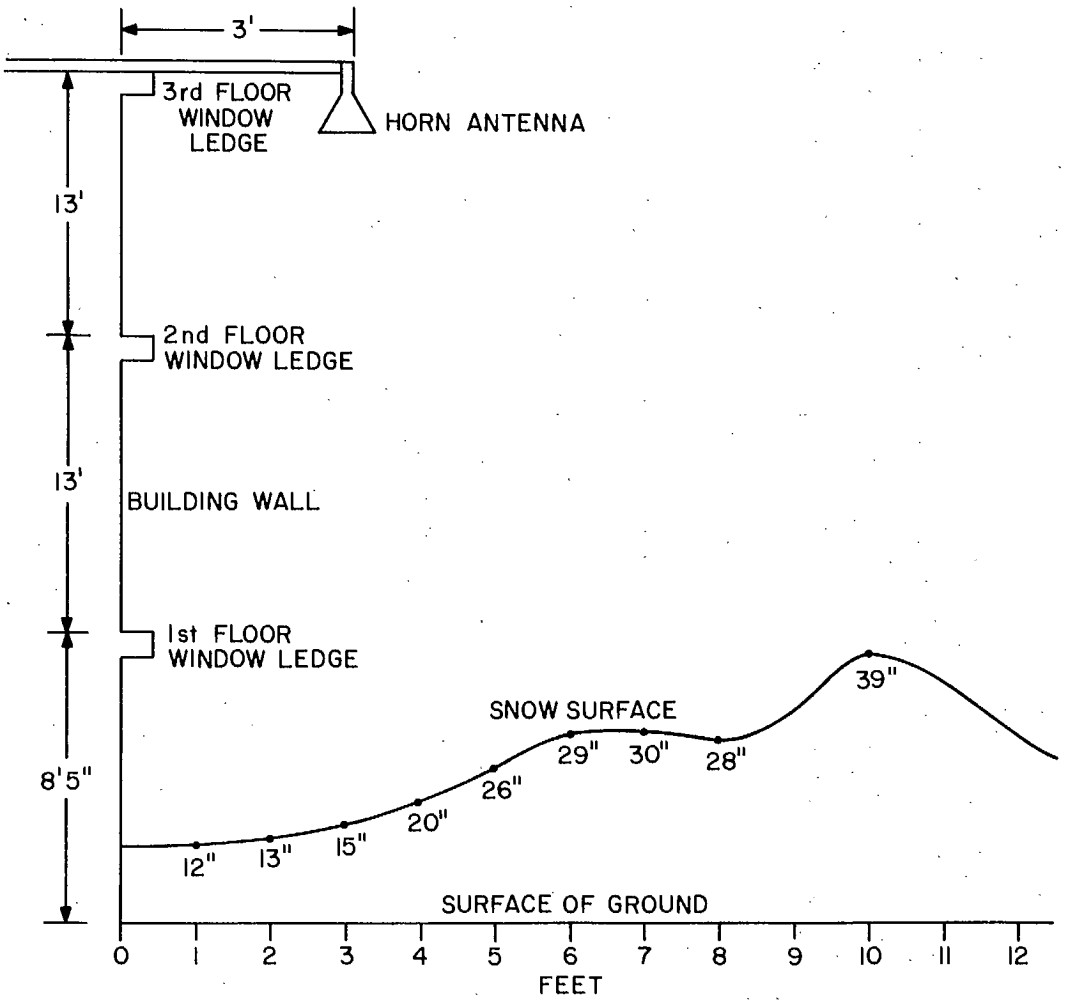

Fig. 5. Snow depth contour beneath window-mounted antenna.

3. CALCULATION OF REFLECTION COEFFICIENT

If it is assumed that the reflection from the surface is specular and the surface flat, the reflection coefficient may be calculated from the geometry shown in Figure 7. The signal is considered to be radiating from the image horn and received by the real horn. If the surface were a perfect reflector the received power would be given by

$$P_s = \frac{P_T \, G \, A_a}{4\pi (2R_s)^2} \, .$$

where P_T = transmitted power

G = antenna gain

A_a = antenna aperture.

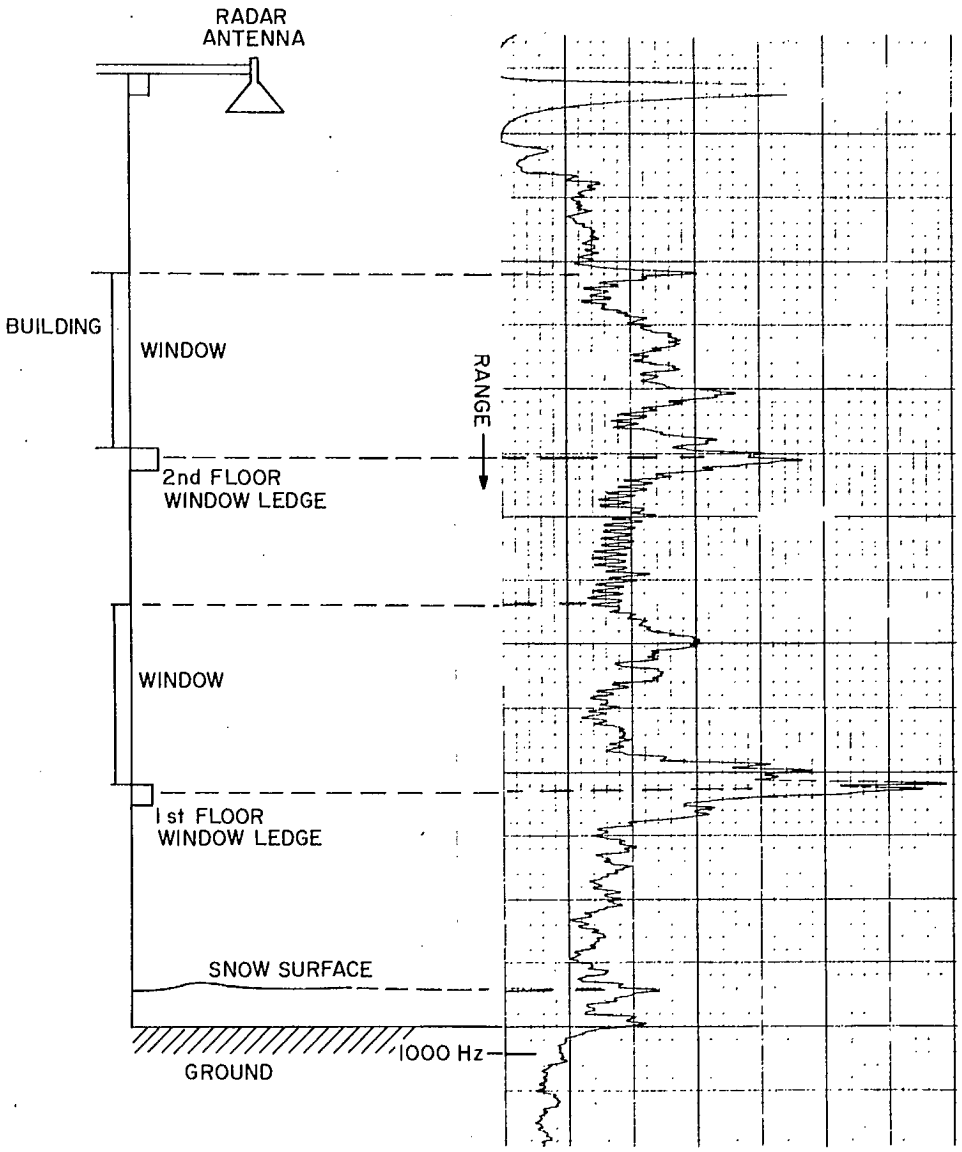

Fig. 6. Data record of the snow, ground and laboratory windows.

When the surface is not a perfect reflector but has a reflection coefficient ρ the received power becomes

$$P_s = \frac{P_T\ G\ A_a\ |\rho|^2}{4\pi(2R_s)^2} \quad . \qquad .....(1)$$

Consider also the power which would be received from a reflector of radar cross section σ_r at range R_r, which is

$$P_r = \frac{P_T\ G\ \sigma_r\ A_a}{16\pi^2 R_r^4} \quad . \qquad .....(2)$$

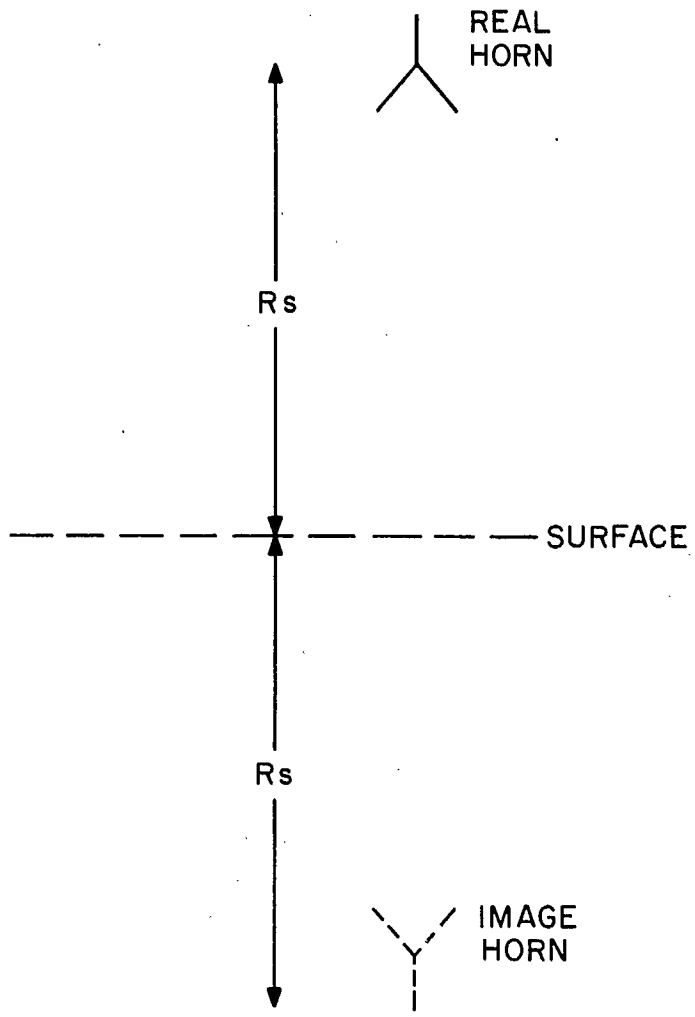

Fig. 7. Geometry for calculation of reflection coefficient.

Taking the ratio of power received from the surface to power from the reflector we have

$$\frac{P_s}{P_r} = \frac{\pi \, |\rho|^2 \, R_r^{\,4}}{\sigma_r R_s^{\,2}} \quad ,$$

from which

$$|\rho| = \frac{R_s}{R_r^{\,2}} \left[\frac{P_s}{P_r} \quad \frac{\sigma_r}{\pi}\right]^{\frac{1}{2}} .$$

If our system has output voltages V_s for the surface and V_r for the reflector, proportional to the square root of the received power, then

$$|\rho| = \frac{\sqrt{\sigma_r} \; V_s \; R_s}{\sqrt{\pi} \; V_r \; R_r^{\,2}} \quad . \qquad \ldots\ldots(3)$$

To determine the reflection coefficient $|\rho|$ therefore, we measure the output voltage V_r at range R_r for a reflector of known cross section σ. Then the voltage V_s for the surface at range R_s is measured and $|\rho|$ is calculated from (3).

To compute the reflection coefficient of a second interface such as the snow-earth interface, we must first find the reflection coefficient of the air-snow interface and the loss in the snow. Since the latter cannot be determined from the radar measurement, we will define an 'effective reflection coefficient' for the snow-ground interface which includes this loss. This is the reflection coefficient which would give the measured return when the transmission loss in the snow is zero. This coefficient will always be less than the true coefficient and will depend on the snow depth.

Consider Figure 8 where

ρ_1 = reflection coefficient of air-snow interface (incident signal in the air),

ρ_e = reflection coefficient of snow-earth interface (incident signal in the snow),

t_{as} = transmission coefficient of air-snow interface (incident signal in air),

t_{sa} = transmission coefficient of snow-air interface (incident signal in snow),

E_1 = the magnitude of the field intensity of the signal from the antenna on the air side of the air-snow interface,

E_e = the magnitude of the field intensity of the signal scattered from the earth, on the air side of the air snow interface.

The ratio E_e/E_1 is given by

$$E_e/E_1 = |t_{as}|\ |\rho_e|\ |t_{sa}|.$$

It can be shown that

$$t_{as} = 1 + \rho_1 ,$$

$$t_{sa} = 1 - \rho_1 .$$

Therefore,

$$E_e/E_1 = |1+\rho_1|\ |\rho_e|\ |1-\rho_1| ,$$

from which

$$|\rho_e| = (E_e/E_1)/|1-\rho_1^2| ,$$

$$= |\rho'|/|1-\rho_1^2| . \qquad .....(4)$$

where

$$\rho' = E_e/E_1 .$$

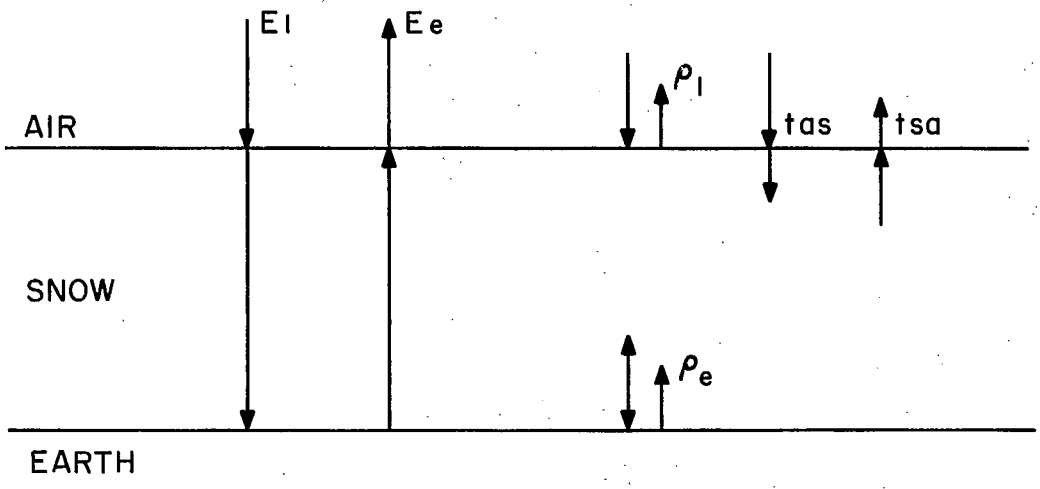

Fig. 8. Measurement of the reflection coefficient of the earth.

If there are layers in the snow giving interfaces with reflection coefficients ρ_2, ρ_3, ..., ρ_n, then it is easily shown that

$$|\rho_e| = \frac{|\rho'|}{|1-\rho_1^2||1-\rho_2^2|, \ldots\ldots, |1-\rho_n^2|} \quad \ldots\ldots(5)$$

Another parameter describing the reflectivity of the surface is the ratio of the measured radar cross-section of the surface area illuminated to the actual area illuminated. The measurement of this ratio, usually referred to as σ^0, does not depend on any assumptions about the specularity of the reflection. For vertical sounding the illuminated area will be approximately

$$A_s = R_s^2 \, \Omega \, ,$$

where R_s = the range to the surface, and

Ω = the solid angle in antenna beam.

Let σ_s be the radar cross section of the illuminated area and σ_r the radar cross section of a known reflector at range R_r. Then from the radar equation (Equation 2), the ratio of received power from the surface to received power from the reflector is

$$\frac{P_s}{P_r} = \frac{\sigma_s}{\sigma_r} \times \frac{R_r^4}{R_s^4} \, ,$$

and

$$\sigma_s = \frac{P_s}{P_r} \, \frac{R_s^4}{R_r^4} \, \sigma_r \, .$$

By definition

$$\sigma^0 = \frac{\sigma_s}{A_s} ,$$

$$= \frac{P_s R_s^2 \sigma_r}{P_r R_r^4 \Omega} ,$$

$$= \frac{V_s^2 R_s^2 \sigma_r}{V_r^2 R_r^4 \Omega} . \qquad .....(6)$$

For the horn used in the experiments,

$$\Omega = .079 \text{ steradian}$$

and

$$\sigma^0 = 12.7 \frac{\sigma_r V_s^2 R_s^2}{V_r^2 R_r^4} . \qquad .....(7)$$

It can be seen that this is the same as ρ^2 in Equation (3) except for a constant which depends on the antenna beamwidth (σ^0 is defined as a power ratio and ρ as a voltage ratio).

4. RESULTS OF SNOW DEPTH MEASUREMENTS

Snow depth measurements were made at two locations. The first ones were made from the Laboratory window from a height of about 35 feet. The equipment was later moved to another area where the antenna was only about eight feet above the surface.

The first series of measurements was made on 7 March 1972 with the set-up shown in Figure 5. The snow depth was slightly less than that shown in Figure 5 since some thawing occurred before the depth measurement was made on 8 March. The temperature was around 25°F and the snow was granular with a grain size estimated at about 1/16 inches and a density of about 0.26 times that of water.

Figure 9 shows the return when a Luneberg lens was placed on the snow surface to provide an accurate range and amplitude reference point. The lens shows up as a strong reflection about 6½ divisions (6½ feet) beyond the first floor window ledge. The lens was on the snow about four feet from the wall where the snow depth was about 26". Thus, we would expect the ground position to be about 9½ divisions beyond the window ledge, allowing for a slightly lower propagation velocity in the snow. A fairly strong reflection at this distance can be seen in Figure 10, which was obtained with the lens removed. Smaller reflections can also be seen above the ground, from the surface of the snow. Some return can be seen slightly ahead of the expected surface position as defined by the lens. This is probably due to reflection from the higher snow further from the building. A reflection can also be seen about one foot beyond the lens position. Since this range corresponds to the snow surface close to the building, it is more likely to be due to a reflection from this surface than to an internal reflection in the snow.

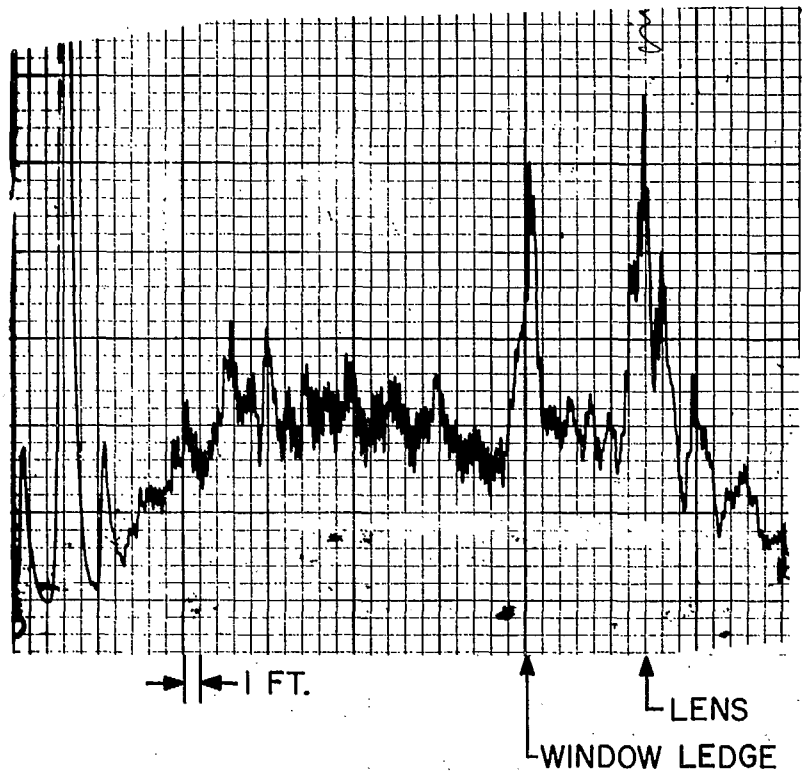

Fig. 9. Data record of a Luneberg lens on the snow surface (laboratory location).

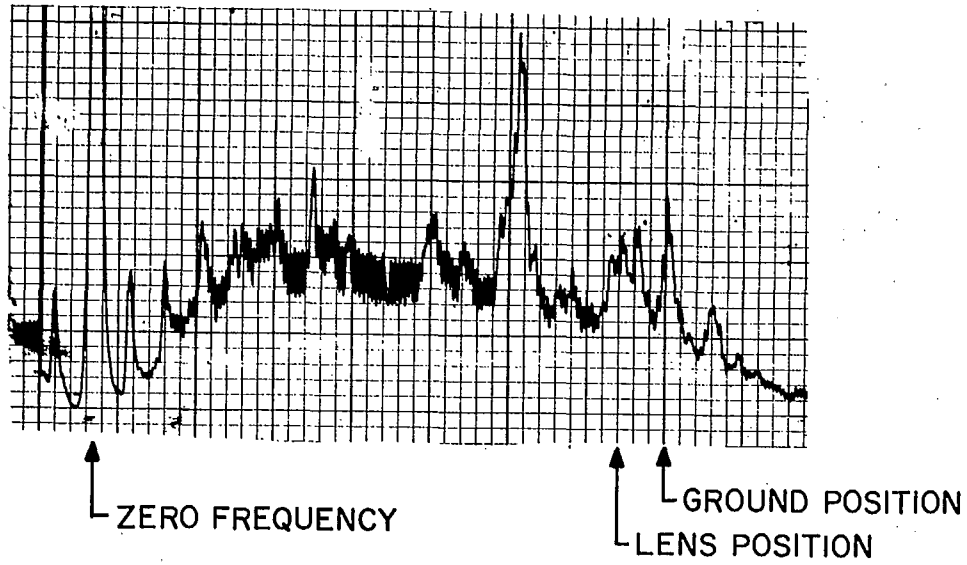

Fig. 10. Data record of the snow and ground surfaces (laboratory location).

From the amplitude of the lens return and the snow and ground returns a reflection coefficient of about 0.10 and a σ^0 of -4 dB were computed for the snow surface and an effective reflection coefficient (as defined in Section 3) of 0.18 was computed for the snow-ground interface.

Figure 11 shows the return during the evening of the same day after a sudden thaw and rain. The return from the wet snow is somewhat increased. This is to be expected as water has a much higher dielectric constant than snow. But the most notable difference is the apparent lack of a return from the ground. This is believed due to the high attenuation of the radar wave in the water contained in the snow. Although the ground return is reduced under these conditions there may still be a significant return which is not detectable in this case due to masking by the strong snow return about one foot away. It is estimated than an effective reflection coefficient of at least 0.04 would be required to allow detection of the ground return under these conditions. Since the multiple snow returns are still present, it is fairly certain that these are caused by the surface at different heights rather than from within the snow. The strongest return from the snow surface indicates a reflection coefficient of about 0.21 and a σ^0 of +2.4 dB.

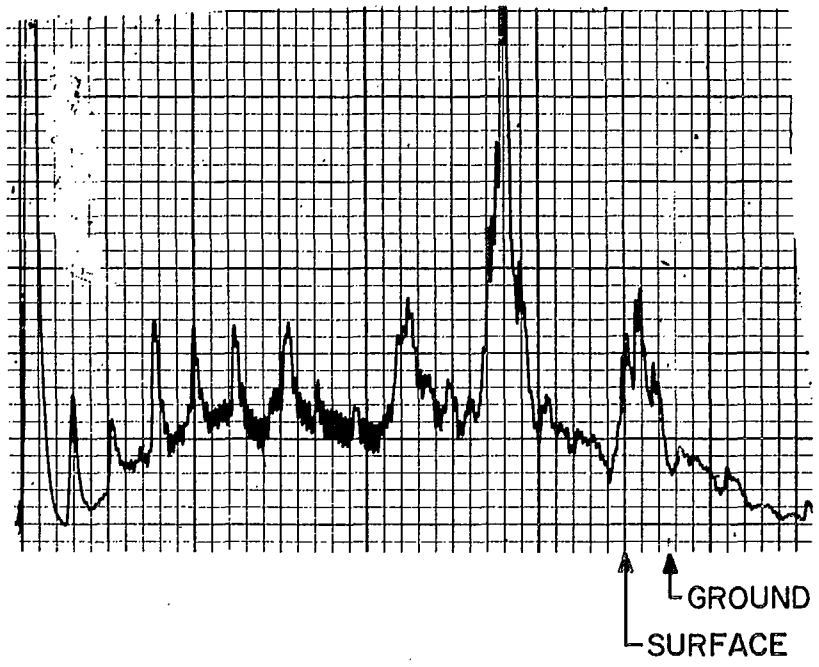

Fig. 11. Data record of the snow and ground surfaces during rain (laboratory location).

A measurement made the following day (Figure 12) after the temperature had again dropped below freezing, shows a reappearance of the ground return with an effective reflection coefficient of 0.14. The returns from the higher snow levels have nearly disappeared, possibly due to the smoother surface from the refrozen crust causing a more specular reflection and directing the beam away from the antenna. The return from the surface at greater range, nearer the building, where the beam would be more nearly normal, is quite strong with a reflection coefficient of about 0.13. There may have been some

slight surface melting due to the sun on the snow since a measurement carried out later when the area was in shadow indicated a reflection coefficient of only 0.11.

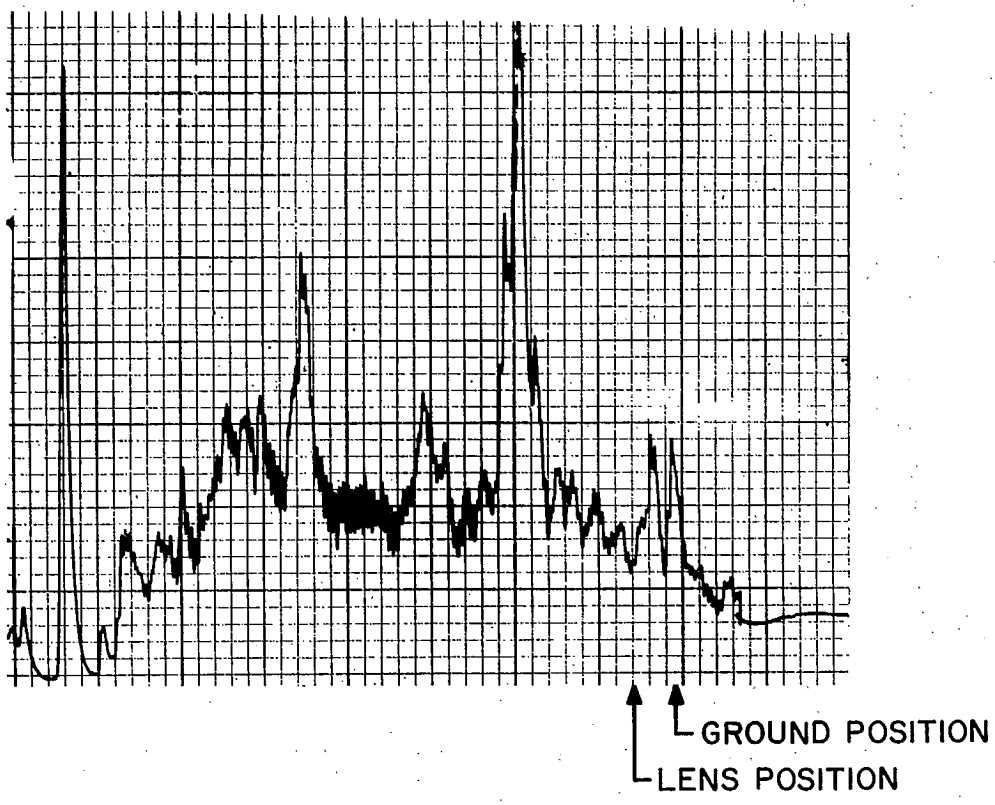

Fig. 12. Data record of the snow and ground surfaces, temperature below freezing (laboratory location).

To increase the accuracy and controllability of the measurements, the radar system was moved to a new location where the horn could be suspended about eight feet above the snow surface, with the nearest reflecting structure well outside the nominal antenna beamwidth. The wide band detector was replaced by a narrower band PRD 601 detector at this point. The combination of this detector and the RF filter reduced the bandwidth slightly below 1 GHz. The bandwidth reduction degraded the resolution slightly but since the range sidelobes were also reduced, a better overall result was achieved. The pen recorder speed was doubled over that used previously to give an expanded scale of about two divisions per foot of range. Figure 13 shows the result of a measurement made with these changes on 13 March. The snow depth was 28 inches and the temperature slightly below freezing. Some thawing had occurred the previous day, and the density of the granular snow had increased to about 0.38 times that of water. A layer of ice three of four inches thick covered the ground under the snow. Two fairly distinct returns, separated by an apparent range of almost three feet can be seen. The lower velocity of the radar wave in the snow accounts for the difference between apparent depth and true depth. The delay per unit distance in snow will depend on the snow density and should vary between about 1.05 and 1.4 times the free space delay.

There is some evidence of possible reflections from within the snow at slightly greater range than the surface return. This may be due, however, to reflections from the surface at points away from the vertical, where the slant range is greater. The returns at ranges greater than the ground range are from a building and other structures outside the nominal beamwidth which have sufficient cross-section to produce a signal return.

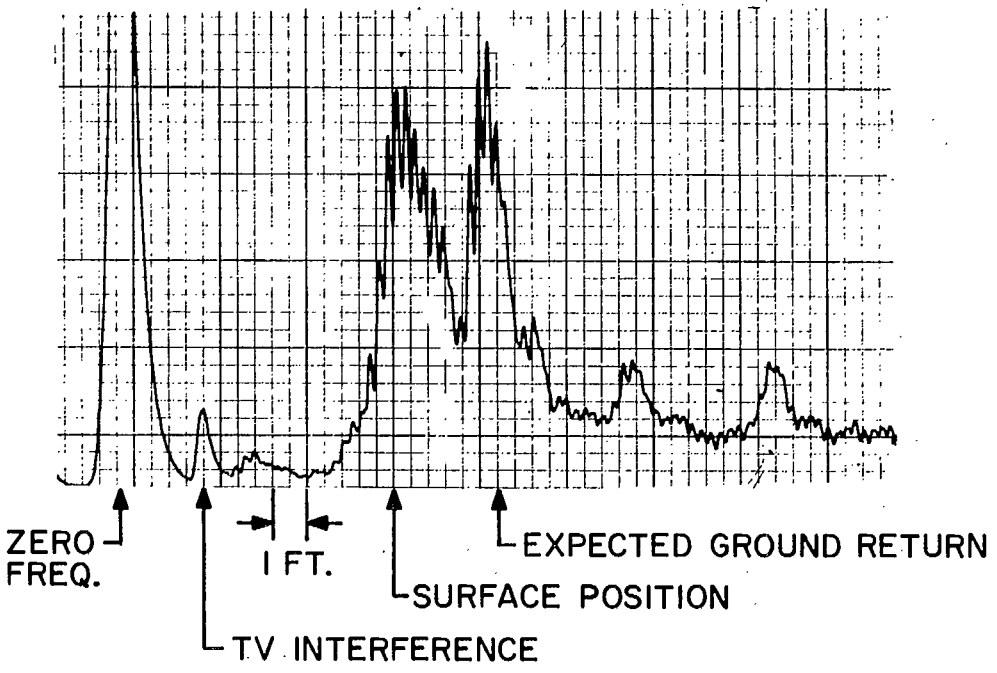

Fig. 13. Data record of the snow and ground surfaces, temperature 30°F (remote location).

The reflection coefficient of the snow surface was found to be about .07 and σ^0 about -7 dB. The effective reflection coefficient of the ground was about 0.10.

Figure 14 was obtained the next day, which was somewhat colder with a temperature of about 15°F. The ground return has been reduced and there is stronger evidence of reflection from within the snow. From Figure 14, the snow surface was found to have a reflection coefficient of about 0.09 and a σ^0 of -5 dB, and the ground was found to have an effective reflection coefficient of about 0.05. The amplitude of the recorder for different tests cannot be compared directly since gains were changed from time to time. However, for each test a calibration measurement was made by placing a reflector of known radar cross-section on the surface. Calculations of reflection coefficient were made using this as a reference.

Figure 15 was recorded on the morning of 15 March at a temperature of 28° F with the antenna moved slightly and illuminating a different patch of snow, although in the same area. Snow depth was 28 inches as before. The ground return has increased again but appears somewhat more spread out, with returns a few inches in front of the expected ground position. This could possibly be due to a change in the snow conditions near the ground or to the layer of ice covering the ground, although the range of these returns makes

the latter interpretation unlikely. The tailing off of the returns beyond the ground position may be due to reflections from the ground away from the vertical or possibly to multiple reflections between the ground and some interface above it, such as the ice surface. The snow surface was found to have a reflection coefficient of 0.10 and a σ^0 of -4 dB. The effective reflection coefficient of the ground was about 0.12.

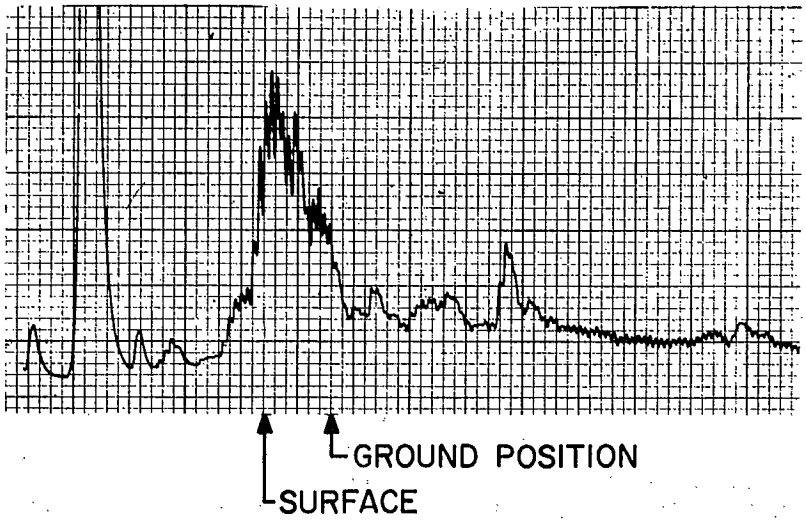

Fig. 14. Data record of the snow and ground surfaces, temperature 15°F (remote location).

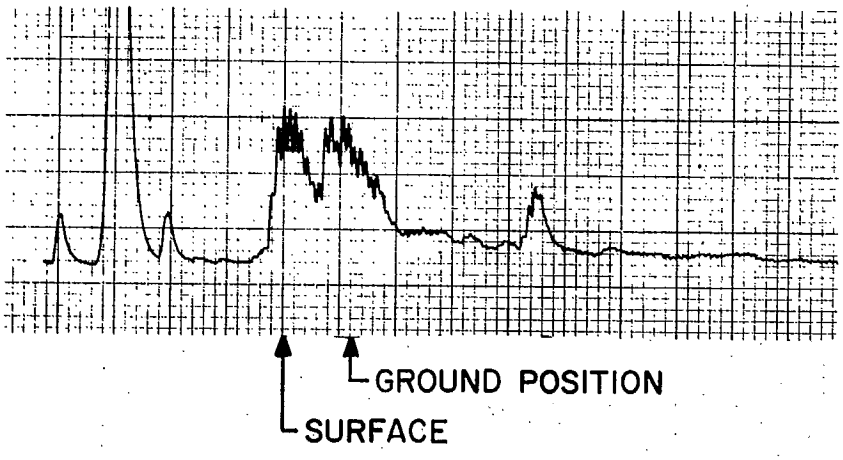

Fig. 15. Data record of the snow and ground surfaces, temperature 28°F, antenna adjusted vertically (remote location).

A measurement was made late on the same afternoon after the sun had caused the surface to become moist. This is shown in Figure 16. The return from the surface has increased, indicating a reflection coefficient of 0.17 and a σ^0 of 0 dB, while the effective reflection coefficient of the ground has decreased to 0.07.

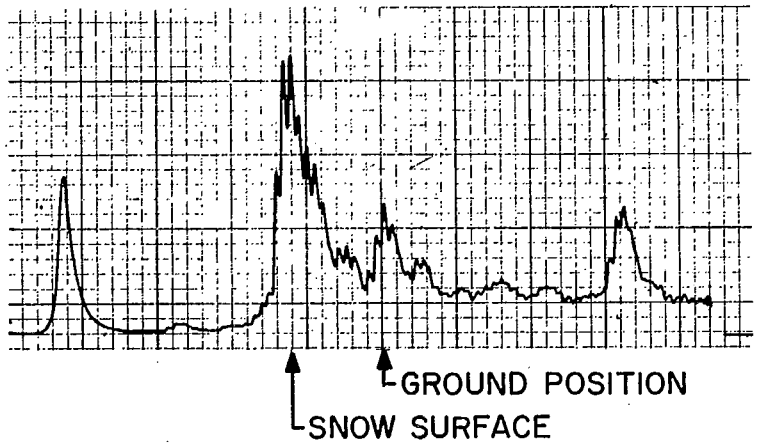

Fig. 16. Data record of the snow and ground surfaces, snow melting, (remote location).

On 17 March, the snow was considerably more moist with the temperature above freezing and a light rain falling. The surface snow had a density of about 0.5 times that of water. The results for this day are shown in Figure 17, which indicates a very strong return from the wet surface (reflection coefficient = 0.25 and σ^0 = +4 dB). The ground return, although considerably weaker than that from the surface, is still clearly visible (reflection coefficient = 0.06). This indicates that the attenuation through the wet snow is not excessive. The reason that the ground return is visible here while not in Figure 11 where conditions were similar may be that the snow was deeper here, moving the ground return farther from the snow return. The signal-to-noise ratio was also higher in this case.

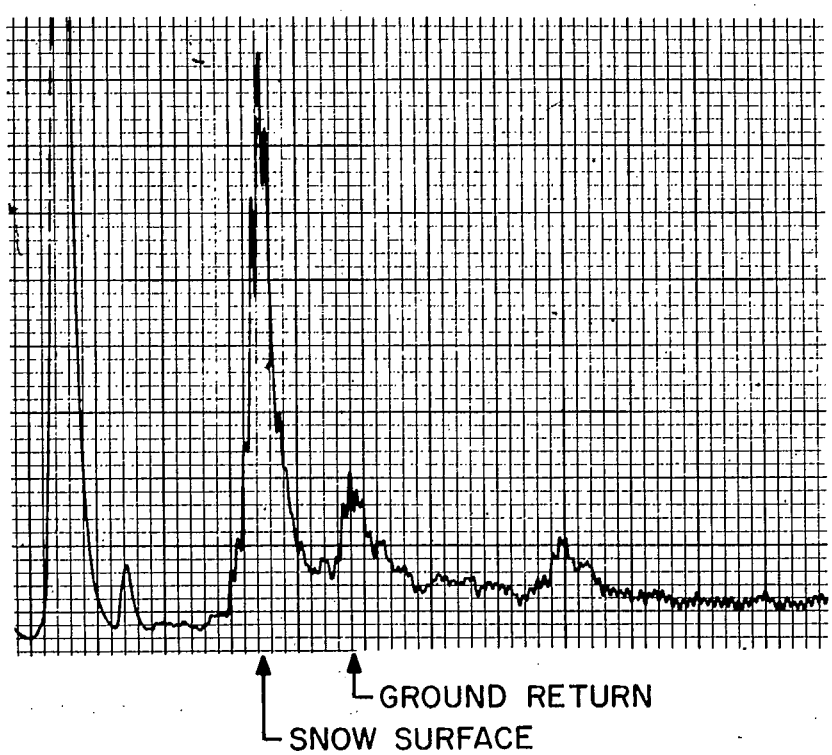

Fig. 17. Data record of the snow and ground surfaces. Raining. (remote location)

4.1 SUMMARY OF RESULTS (SNOW DEPTH MEASUREMENTS)

Measurements were made on relatively dense snow only. Densities in the range 0.3 to 0.4 g/cm^3 gave measured reflection coefficients around 0.1 when the snow was dry. This is in good agreement with theoretical values. When the snow was wet, the reflection coefficient increased to as high as 0.25. During the time of the measurements, there was no snow that was typical of new fallen snow available. It is expected that such snow would have a density of about 0.1 g/cm^3 and a reflection coefficient of about 0.03.

In some measurements there was evidence of reflections from within the snow volume; these may be from interfaces between layers or from density gradients. Scattering from the snow and ice granules does not appear likely due to their small size and close packing. Such reflections should not prevent a determination of snow depth, although a strong reflection near the surface may mask a layer of very light snow on the surface and thus give a low reading of depth.

The ground beneath the snow gave effective reflection coefficients varying from about 0.18 to 0.06, the low values corresponding to the cases where the snow was quite wet. In only one measurement was the ground return not detected. In this case the snow was very wet and conditions were such that it was only possible to say that the effective reflection coefficient was less than 0.04. It is not known what part the three or four inch layer of ice beneath the snow played in the ground reflection, since such a thickness is beyond the resolution capability of the radar. It would be expected that the reflection coefficient of the snow-ground interface would vary over a considerable range depending on soil type, moisture content, density of the snow, etc. However, it would seem reasonable to expect a value of at least 0.01 for all but the most exceptional conditions.

Multiple reflections between the ground and interfaces within the snow, including the snow-air interface, can produce returns at apparent depths greater than that of the ground. Such returns would be small compared to the ground return but they might confuse the picture in some cases. In only a few measurements did evidence of this effect occur and even then, it was not certain that multiple reflections were the cause.

5. RESULTS OF ICE THICKNESS MEASUREMENTS

Ice thickness measurements were carried out on the Jock River near the village of Richmond. The radar antenna was attached to the railing of a bridge at the approximate centre of the span as shown in Figure 18. An end view of the bridge section is shown in Figure 19. At a point directly under the antenna, the total ice thickness was 36 inches. This included 14 inches of white opaque ice at the top and 22 inches of clear ice at the bottom. There was approximately 15 feet of water beneath the ice.

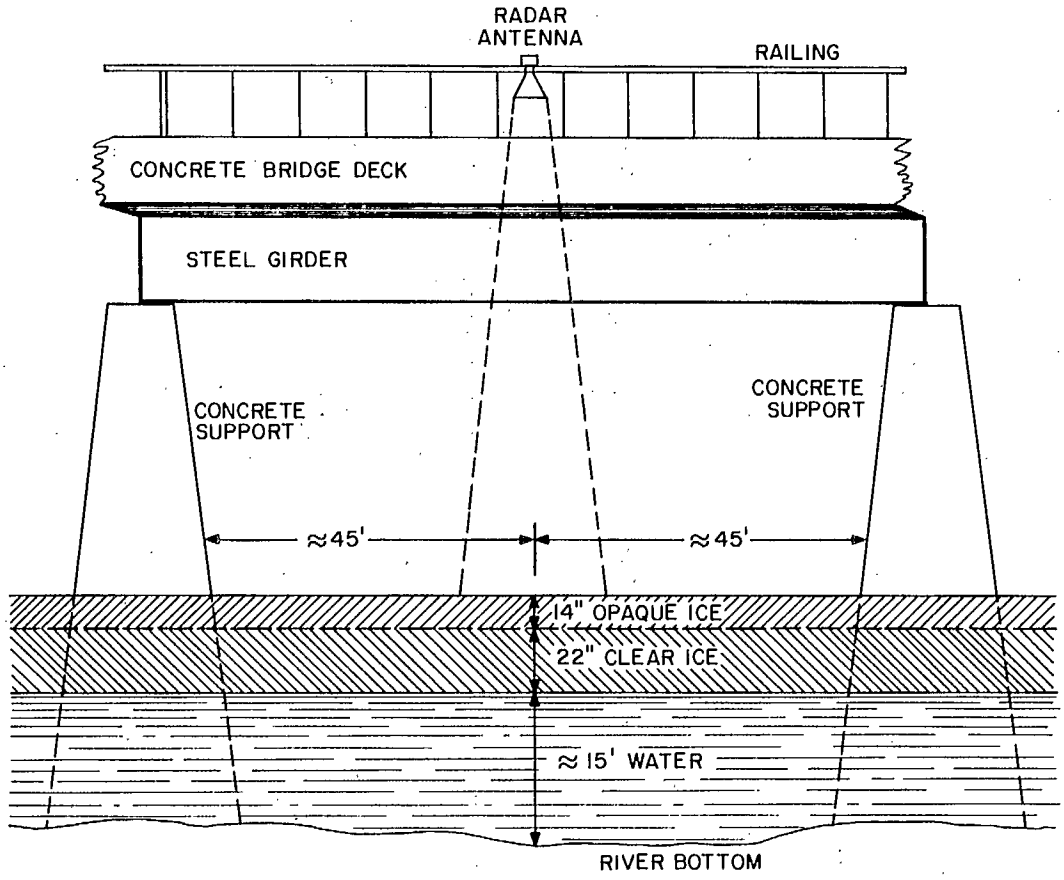

Fig. 18. Bridge section (front view).

With the antenna mounted on the bridge railing, approximately 18.5 feet above the ice, the radar was calibrated by placing a reflector of known radar cross-section on the ice-surface as described in Section 4. The results of the first ice-thickness measurements are given in Figure 20. The target at 'A' was the ice surface and the smaller target at 'B' was assumed to be from the surface of the water under the ice. The reflection coefficient of the ice surface was computed to be 0.14 and σ^0 was -1 dB. The effective reflection coefficient of the ice-water interface was only about 0.002. Each small division on the plot was equal to a range of six inches. Thus, since there were approximately 11 small divisions between targets 'A' and 'B', the range between the two targets was 5.5 feet (i.e., target separation of 5.5 feet). However, the propagation velocity of X-band microwaves through ice is only .56 of their velocity in free space; therefore, the ice thickness measured by the radar was approximately 37 inches. The target shown at 'C' may be due to reflections from the interface between the opaque ice and the clear ice. The target shown at 'D' is believed to be a reflection from the steel girders of the bridge.

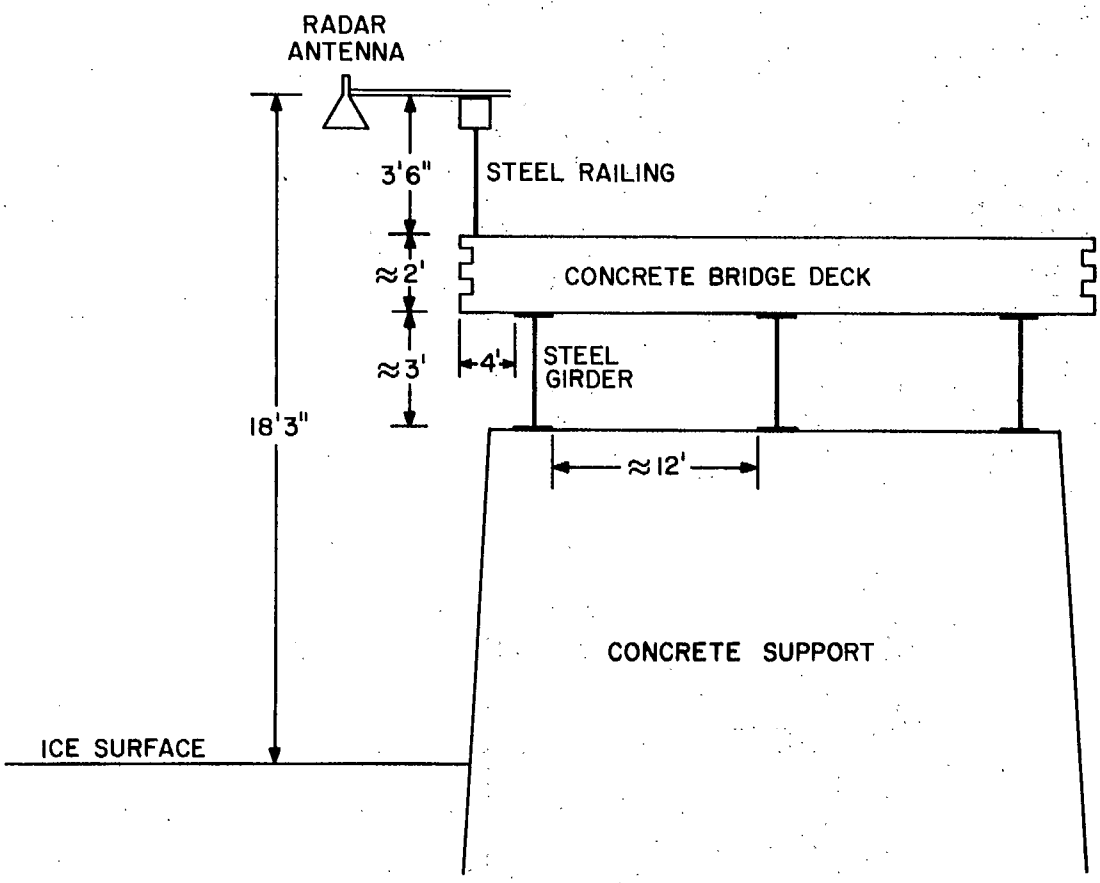

Fig. 19. Bridge section (end view).

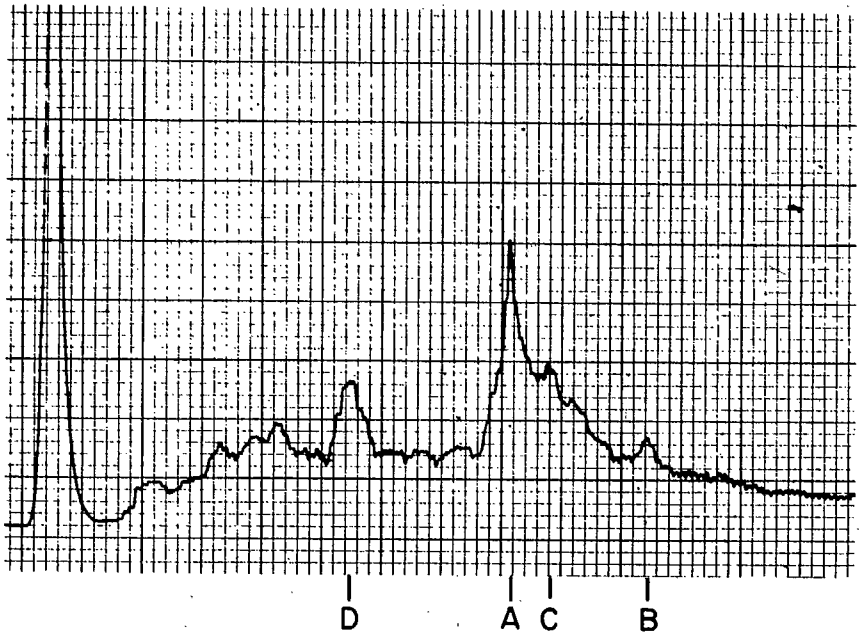

Fig. 20. First ice thickness data record.

Figure 21 shows the results of another measurement about a half hour later on the same day. The strongest reflection at 'A' now occurs about six inches below the ice surface (as determined by the radar reflector on a previous measurement), and there is evidence of the return from the surface just ahead of the maximum. The top six inches of ice appeared slightly softer than the rest and a change in dielectric constant at the interface between this and the ice below could account for the strong reflection from this level, indicating a reflection coefficient of 0.14 (the same as that of the surface in Figure 20). However, it is not clear why the surface reflection has been reduced relative to that in Figure 20, and the below-surface reflection increased. The temperature was around 15°F but the sun may have had some effect on the surface. The measurements were made in the early afternoon and the sun would be slightly lower for the second measurement. The effective reflection coefficient of the ice-water interface was found to be 0.004. The reflection from the interface between the opaque and clear ice was not as evident in this figure, but this is probably due to increased masking from the strong return which is closer than in Figure 20.

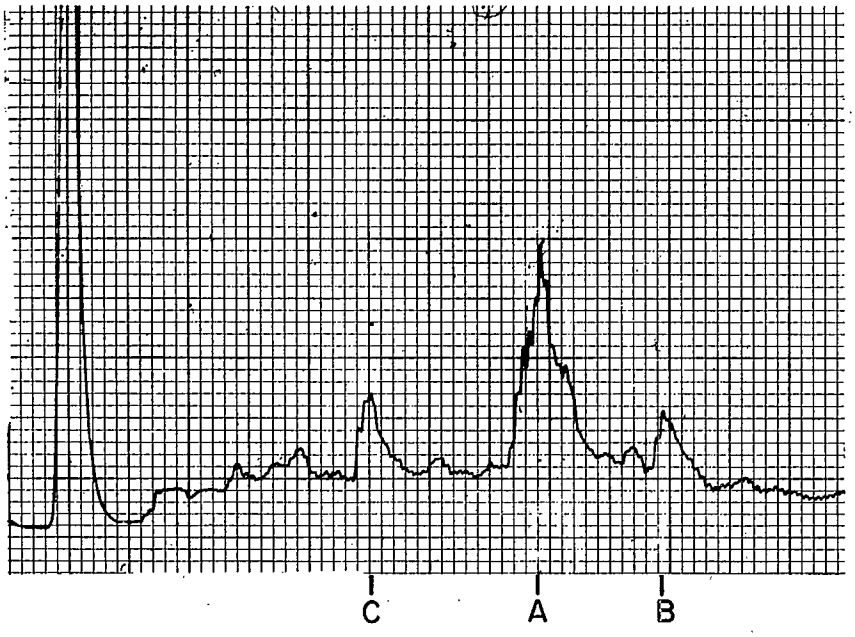

Fig. 21. Second ice thickness data record.

After the ice-thickness measurements were completed, a hole, 28 inches by 18 inches, was chopped through the ice to verify the radar measurements. The water level in the test hole rose to within six inches of the ice surface. A radar measurement was carried out and the resultant plot is shown in Figure 22. The reflection coefficient of the water was found to be 0.5 and the value of σ^0 was +11.2 dB. These figures are based on the assumption that the water surface intercepted all of the energy which would return to the antenna from specular reflection. Since the hole was not very large, and its center may not have been directly below the antenna, this may not be true. The difference between the measured reflection coefficient and the theoretical value of 0.74 may be due to the inaccuracy of this assumption. If the radar

range of the ice surface (point 'A', Figure 20) is compared with the radar range of the water surface in the test hole (point 'A', Figure 22), it may be seen that the ice surface was approximately six inches closer to the radar than the water surface. As stated previously, the water surface in the test hole was six inches below the ice surface; therefore, this measurement verified the accuracy of the radar range measurements.

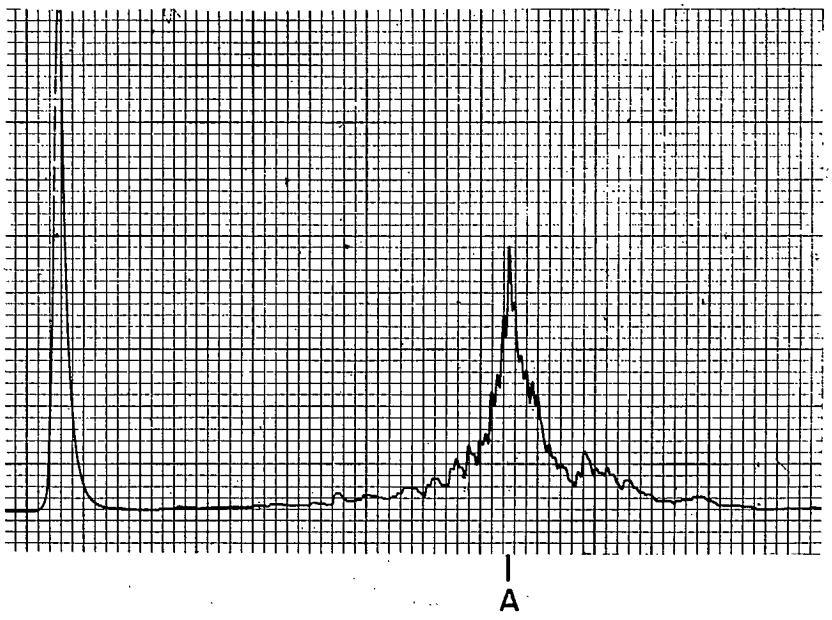

Fig. 22. Data record of the water surface.

5.1 SUMMARY OF RESULTS (ICE THICKNESS MEASUREMENTS)

The very low effective reflection coefficient of the ice-water interface (.002 to .004) was rather surprising. The theoretical coefficient is about 0.66. Since our measurements did not take the attenuation in the ice into account, we would expect our measured values to be somewhat lower than this. But the expected attenuation is less than 2 dB, which would only reduce the coefficient by about 20%. This great discrepancy can be attributed to one or both of two possible causes - that the attenuation in the ice is actually very much greater than expected, or that the reflection coefficient is actually very low. The first cause implies a loss in the ice of more than 40 dB. While there is some possibility of increased attenuation due to contamination from salf used on the bridge above, it does not seem likely that this could account for such high attenuation.

The second cause may result from a gradual change in permittivity between the water and the ice. The temperature of the water below the ice was probably well above freezing, and melting would be taking place at the lower ice surface. In making the hole, it was found that the ice began to get wet and slushy a few inches above the bottom surface of the ice (i.e., before breaking though to the water below). The presence of this liquid water in the ice, presumably decreasing in percentage with height, could, it would seem, cause a gradual permittivity change resulting in a quite low reflection coefficient. The very limited program of measurement undertaken up to this time was not sufficient to resolve this point with any degree of certainty.

However, it appears that sufficient reflection does occur at the ice-water interface to allow ice thickness measurement. It is expected that the reflection would be stronger during the winter but further measurements would be necessary to confirm this.

6. SOME REQUIREMENTS FOR AN AIRBORNE SNOW AND ICE DEPTH MEASURING RADAR

6.1 ANTENNA BEAMWIDTH

If the surface was entirely flat, allowing only specular reflections, all reflections would occur in a very small area directly under the aircraft, and antenna beamwidth would not be important. However, since this is not the case, a narrow antenna beam will be necessary to prevent reflections from surfaces and objects, well away from the point under the aircraft, from entering the system. Such reflections will be at longer range than the surface below the aircraft and will confuse the picture. For a level surface, the increase in slant range to the surface at an angle θ from the vertical will be approximately $\frac{R\theta^2}{2}$, where R is the vertical range to the ground (aircraft altitude). To keep this error less than some maximum allowable error, say d_ε, we must keep θ less than some value θ_m, where

$$\theta_m = \sqrt{\frac{2d_\varepsilon}{R}}$$

For an aircraft altitude of 1000 feet and a maximum allowable error of 0.5 feet,

$$\theta_m = .032 \text{ radians or } 1.8 \text{ degrees.}$$

Thus, to keep range error less than one-half foot the antenna should not radiate significantly over a beamwidth of more than 3.6 degrees. A reduction of altitude to 500 feet would increase the allowable beamwidth to 5 degrees. Therefore for altitudes between 500 and 1000 feet, the 3 dB beamwidth should not be more than one or two degrees. Although altitudes lower than 500 feet are possible with fixed wing aircraft over most terrain, we consider 500 to 1000 feet more typical of reasonable operational altitudes.

6.2 AIRCRAFT SPEED

During the measurement time, the area illuminated should not change significantly. A one degree beam at 1000 feet will illuminate a spot about 17.5 feet in diameter. Thus, the aircraft should not move more than one or two feet during the measurement. For a fixed-wing aircraft, this means that the slow technique used in the experimental system would not work. However, if all the information from one sweep of the RF generator were stored, the spectrum from this could be computed later and it would be necessary only to keep the sweep time short enough. At a speed of 300 ft/sec, a distance of two feet would be covered in about 6.7 milliseconds. Thus, it appears that a

somewhat shorter sweep than that used in the experimental system would be necessary unless a rotary-wing aircraft were used. Such a vehicle would also allow much lower altitudes, and hence ease the antenna requirement.

6.3 TRANSMITTED ENERGY REQUIREMENT

The other factor affecting the sweep time is the transmitted energy requirement. The sweep time must be long enough to provide sufficient energy for detection with the available peak power. The energy requirement may be derived by considering the signal to be radiating from an antenna below the surface at the mirror image point of the real antenna. This situation is depicted in Figure 23. The energy received at a height R_s above the surface, when the surface has a reflection coefficient ρ, will be

$$E_r = \frac{E_T \, G|\rho|^2 A_a}{4\pi \, (2R_s)^2} \qquad .....(8)$$

where E_T = transmitted energy
G = antenna gain
A_a = antenna aperture.

Substituting $A_a = \frac{\lambda^2 G}{4\pi}$ in (8) and computing the signal-to-noise ratio

$$(S/N) = \frac{E_r}{kTN}$$

where k = Boltzmann's constant
T = temperature in degrees K
N = noise factor,

we have

$$(S/N) = \frac{E_T \, G^2 \, |\rho|^2 \lambda^2}{64\pi^2 R_s^2 \, kTN} .$$

The transmitted power required to produce a signal-to-noise ratio (S/N), is therefore,

$$E_T = \frac{2.65 \times 10^{-18} \, R_s \, N \, (S/N)}{G^2 |\rho|^2 \lambda^2} \qquad .....(9)$$

Consider a typical case where

λ = 3 cm. = 0.1 ft
R_s = 1000 ft
G = 40 dB (pencil beam of about 2 degrees)
N = 32 (noise figure = 15 dB).

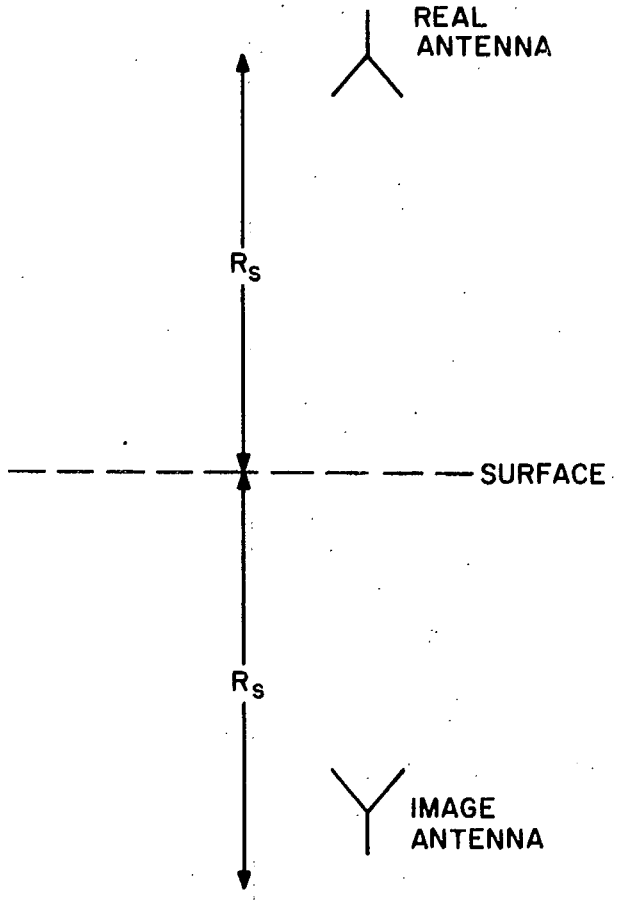

Fig. 23. Geometry for calculation of required energy.

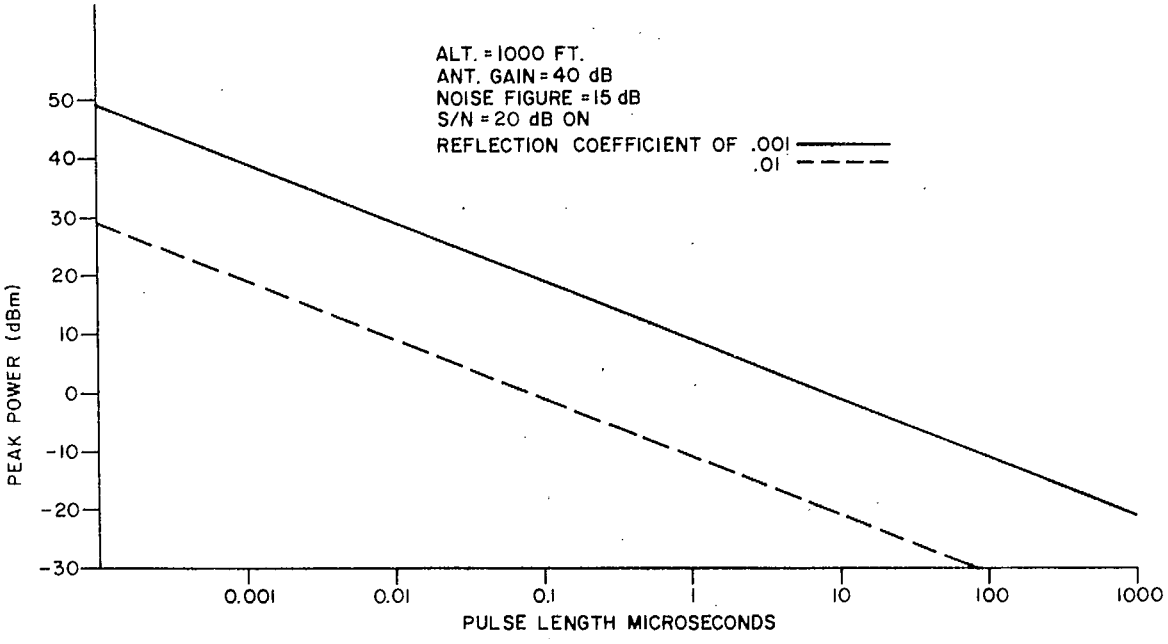

Fig. 24. Power required vs pulsewidth for snow sounding radar.

Also, assume that a signal-to-noise ratio of 20 dB is required on a minimum reflection coefficient of .001. This would seem to be a very conservative requirement. Then

$$E_T = 8.5 \times 10^{-9} \text{ joules.}$$

If integration occurs over a pulse length T_p of constant amplitude, the required peak power is

$$P_T = \frac{8.4 \times 10^{-9}}{T_p} .$$

The required peak power is plotted in Figure 24 as a function of T_p. Also plotted as a broken line is power required for a minimum reflection coefficient of .01 to give a 20 dB signal-to-noise ratio. These curves indicate that only a very short pulse or sweep time is required even for very small peak power.

A pulse length of 0.5 nanoseconds can provide a resolution of about 3 inches without FM. Such a pulse would require a peak power of 16 watts for the conservative case and 150 milliwatts in the less conservative case. Thus, it appears that the required performance may be achieved with a simple short pulse if a pulse of this duration can be generated. However, the difficulties involved in the generation of such a pulse and in display of the received signal may make a simple pulse system more complex and expensive than an FM system.

6.4 BANDWIDTH OF SIGNALS FOR PROCESSING

An advantage of an FM system of the type described is that although a large RF bandwidth is required, the output difference frequency which is to be processed has a relatively small bandwidth. This bandwidth is determined by the range of difference frequencies to be expected for the maximum depth of targets of interest. A depth of 20 feet should be adequate for this purpose. This corresponds to a delay difference of about 40 nanoseconds. The bandwidth of the difference frequency for a delay difference t_d is given by

$$B = \frac{f_s}{t_s} t_d \qquad \text{.....(10)}$$

where f_s is the frequency through which the radar sweeps and t_s is the time for a sweep. We have shown previously that to complete a measurement before the illuminated spot on the surface has moved appreciably, we would require a maximum sweep time of about 6.7 milliseconds for a speed of 300 feet per second. A value of t_s of 5 milliseconds should be about right, therefore, and for a resolution of 3 inches, f_s must be about 2 GHz. Therefore, from (10), B = 16 kHz. Recording of signals of this bandwidth can be accomplished with either analogue or digital magnetic tape. Digital recording would require sampling and analogue-to-digital conversion at a rate of at least 32 kHz.

6.5 EFFECT OF DOPPLER GENERATED BY SLOPING TERRAIN

Sloping terrain will appear to be rising or falling as the aircraft passes over it. This will cause a doppler shift proportional to the slope and the aircraft speed. For a slope of 10° and an aircraft speed of 300 ft/sec the doppler shift will be about 1 kHz at X-band. With the sweep rate given in the last section, this will give a range error of about 1.25 feet. However, in measuring depth it is only the difference between the ranges of the two surfaces which is important and if these are parallel there should be no depth error. Since this is not the case with snow drifts or ice ridges, these may cause some errors.

7. CONCLUSIONS

The work described in this note is intended only as a quick look at the feasibility of using high resolution radar to measure snow and ice depth. The equipment used was fairly crude and the data samples were limited. However, the results are encouraging, and it appears that snow and fresh water ice depth measurement by radar, with a resolution of a few inches, is feasible over quite a range of conditions, with quite low peak power.

With an X-band FM system, although a large RF bandwidth of one or two gigahertz would be required, the bandwidth of the signal to be processed need only be a few tens of kilohertz. Processing of the signal involves spectral analysis and could probably best be done digitally on the ground on signals stored on either analogue or digital magnetic tape. Depth can be determined by inspection of an amplitude vs range plot generated from each RF sweep. However, where continuous data over a long track is desired, automatic computation and plotting of snow and ice depth would probably be necessary. This appears feasible, although secondary reflections may cause inaccuracies in some cases where human interpretation would have resolved them.

Of particular importance for a snow depth measuring radar is the relative amplitude of the returns from the different surfaces. Where there is a great difference, resolution will suffer since shoulders or sidelobes of the return from one surface may mask the return from the other. From the limited measurements made, it appears that for snow covering the ground, this difference is normally not very great. The measurement of ice over water, on the other hand, showed a greater difference with the ice-water interface being unexpectedly the weaker. Measurements were made on only one day, however, and this may have been an exceptional case. In any case, range sidelobes should be kept as low as possible, preferably 30 or 40 dB below the main response.

Although the propagation velocity in snow depends on the snow density, the range of variation is fairly limited, and even a very rough estimate of snow density should allow quite an accurate depth measurement. There should be even less uncertainty with ice. Propagation velocity will depend on temperature which should be fairly well known.

8. ACKNOWLEDGEMENTS

The authors wish to thank Mr. G.M. Royer of the Radar Systems Engineering Section of the Communications Research Centre for information pertaining to the attenuation and reflection of radar signals in ice and snow.